



Supplement of

A simplified non-linear chemistry transport model for analyzing NO₂ column observations: STILT-NO_x

Dien Wu et al.

Correspondence to: Dien Wu (dienwu@caltech.edu)

The copyright of individual parts of the supplement might differ from the article licence.

Site	Emission	NO _x chemistry	Inter-parcel mixing	Meteorological fields	Model-TROPOMI slope	RMSE (mean bias) [ppb]
New Madrid, MO (8 of 34 overpasses in JJA)	EPA (hourly)	Yes	Yes	GFS	1.22 (J-D); 1.03 (JJA)	0.14 (-26%)
	EPA (hourly)	Yes	Yes	GFS	1.21 (J-D); 1.03 (JJA) with background subtracted	0.15 (/)
	EPA (hourly)	Yes	Yes	HRRR	1.24 (J-D); 1.05 (JJA)	0.11 (-4%)
	EPA (hourly)	Yes	No	GFS	1.19 (J-D); 1.01 (JJA)	0.13 (-28%)
	EPA (hourly)	No	Yes	GFS	1.77 (J-D); 1.68 (JJA)	0.25 (40%)
	EDGARv6 (monthly)	Yes	Yes	GFS	0.53 (J-D); 0.16 (JJA)	0.14 (-49%)
Thomas Hill, MO (9 overpasses in JJA)	EPA (hourly)	Yes	Yes	GFS	1.13 (JJA)	
	EPA (hourly)	Yes	No	GFS	1.14 (JJA)	
	EPA (hourly)	No	Yes	GFS	1.86 (JJA)	
	EDGARv6 (monthly)	Yes	Yes	GFS	0.58 (JJA)	
	EDGARv6 (monthly)	No	Yes	GFS	1.24 (JJA)	
Martin Lake, TX (7 overpasses in JJA)	EPA (hourly)	Yes	Yes	GFS	1.29 (JJA)	
	EPA (hourly)	Yes	No	GFS	1.29 (JJA)	
	EPA (hourly)	No	Yes	GFS	2.27 (JJA)	
	EDGARv6 (monthly)	Yes	Yes	GFS	2.03 (JJA)	
	EDGARv6 (monthly)	No	Yes	GFS	3.34 (JJA)	

Table S1. A summary of the model-data slopes averaged over all simulations for each power plant. These values correspond to the horizontal lines in **Fig. 7** with removal of three “outliers” overpasses with significant wind directional biases. The results with the best configurations are outlined by solid black boxes. For the “no” NO_x chemistry simulation, a constant NO₂ -to-NO_x ratio is still applied.

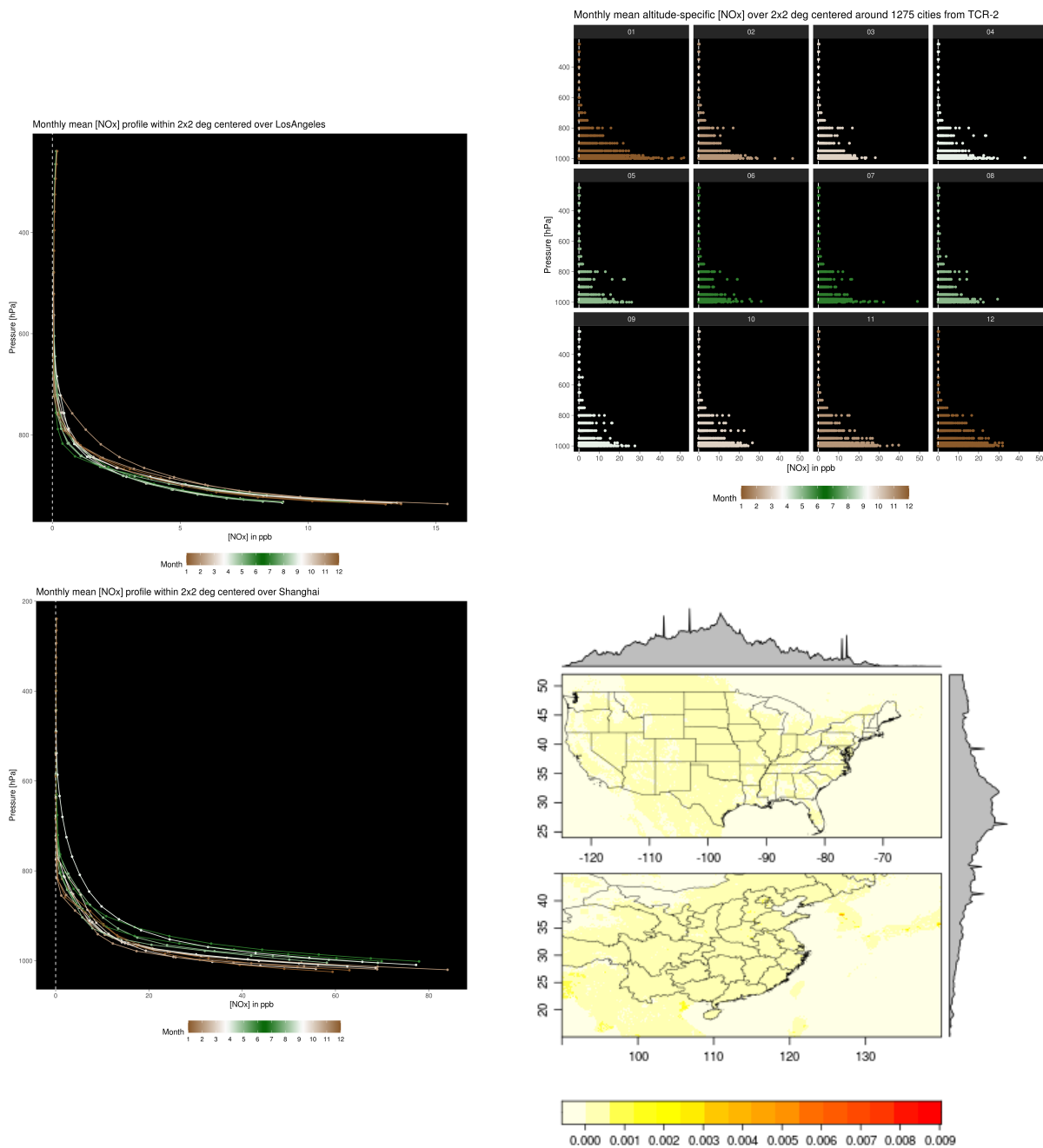


Figure S1. Left panels: monthly average level-specific NO_x mixing ratio [ppb] over 2° by 2° around Los Angeles (upper) and Shanghai (lower). WRF-Chem runs are driven by EDGAR emissions and generated for multiple selected days in a month. Upper right: month average pressure-specific NO_x mixing ratio [ppb] over 2° by 2° areas around thousands of global cities based on TCR-2 reanalysis in 2019. Each dot denotes one pressure level per city. The color gradient represents 12 months. Bottom right: Maps of non-anthropogenic NO_x emissions according to TCR-2.

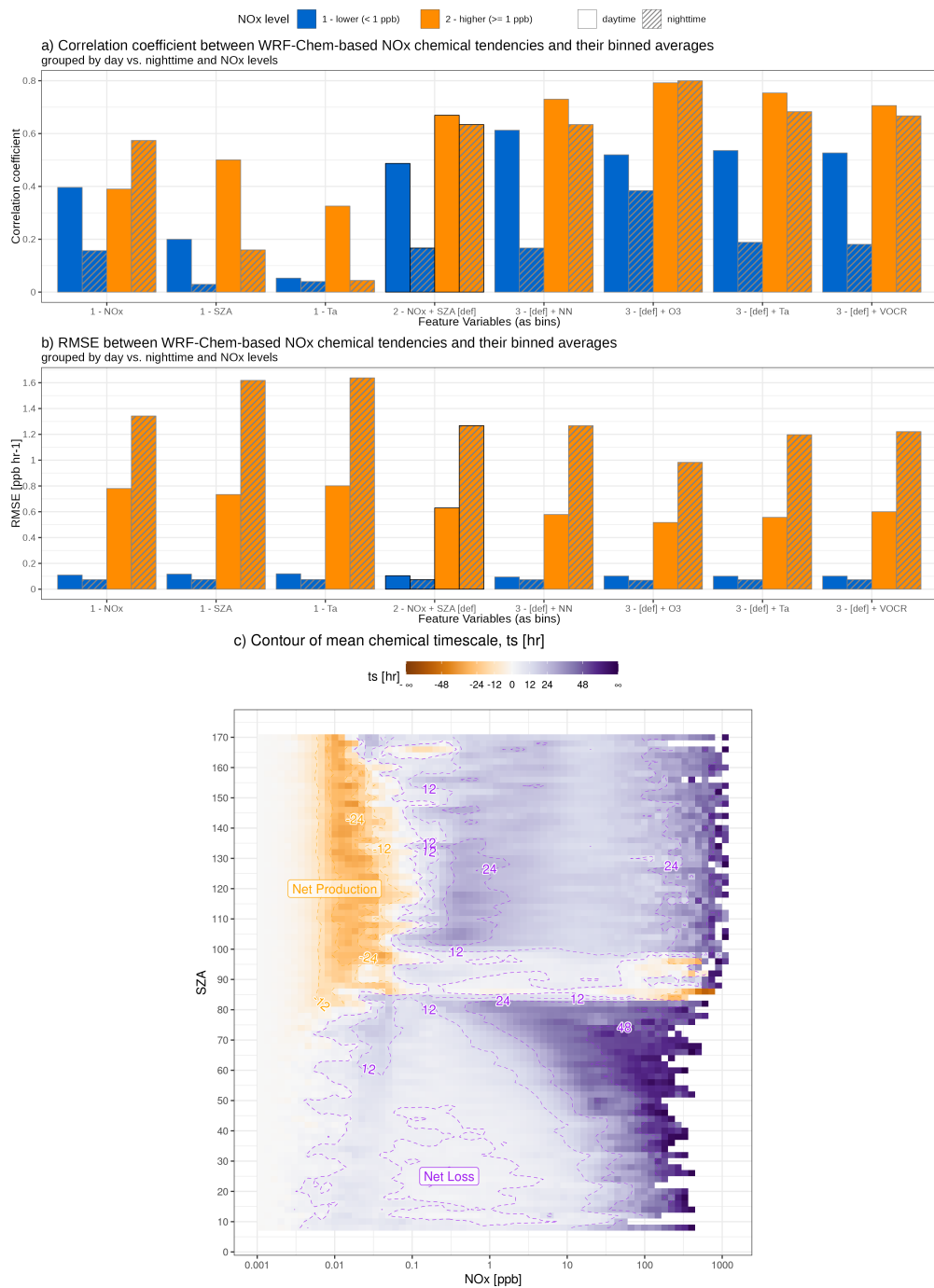
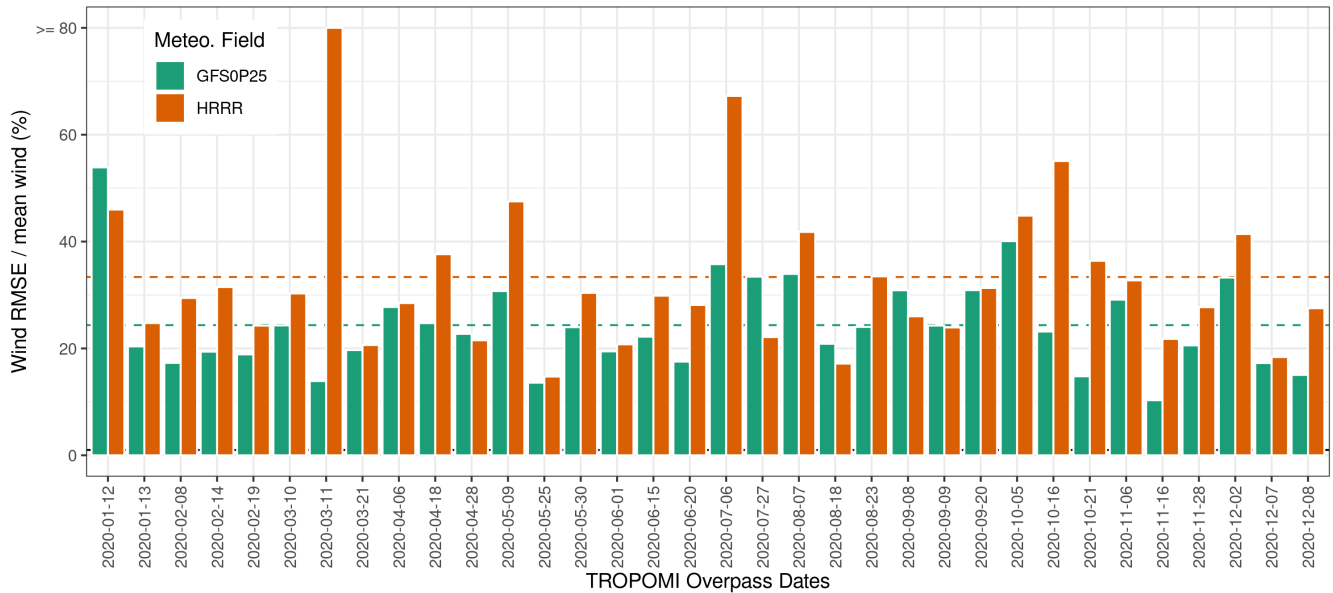


Figure S2. (ab) Correlation coefficient and RMSE between the raw R_{NO_x} directly derived from WRF-Chem and the bin-averaged R_{NO_x} based on 8 combinations of feature variables. The number in front of the feature variables on the x-axis denotes the total number of variables used when grouping the raw R_{NO_x} . The combination we used (2-NO_x+SZA for NO_x concentration and solar zenith angle, SZA) is highlighted in bars with black outlines. Additional variables tested include air temperature (Ta), NO₂-to-NO_x ratio (NN), ozone (O₃), and VOC reactivity (VO_{CR}). Results are reported separately for higher or lower NO_x levels (orange or blue) during the day or night (empty bars or bars with strips). (c) A contour view of the net NO_x loss timescale in hours, summarized for each SZA and NO_x bins, as an extension of Fig. 2b.

Ratio of random wind error over mean wind speed below 2 km
per TROPOMI overpass over available NOAA RAOB sites around NewMadrid



Ratio of random wind error over mean wind speed below 2 km
per TROPOMI overpass over available NOAA RAOB sites around Intermountain

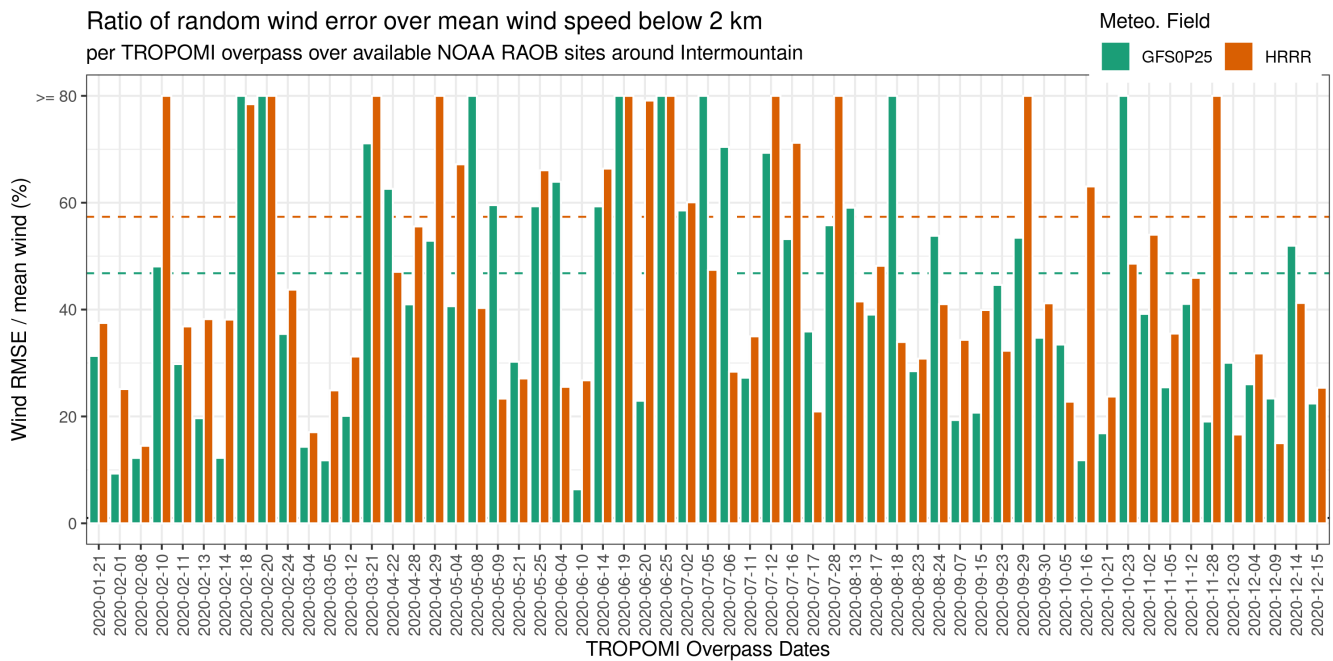


Figure S3. The modeled u/v- component wind from 3km HRRR (orange bars) or GFS0p25 (green bars) are evaluated against measured wind speed from NOAA radiosonde sites based on all available observations around twp power plants, below 2 km during the 24 hours ahead of the TROPOMI overpass time. The random wind error normalized by the mean wind speed [%] is calculated for each overpass.

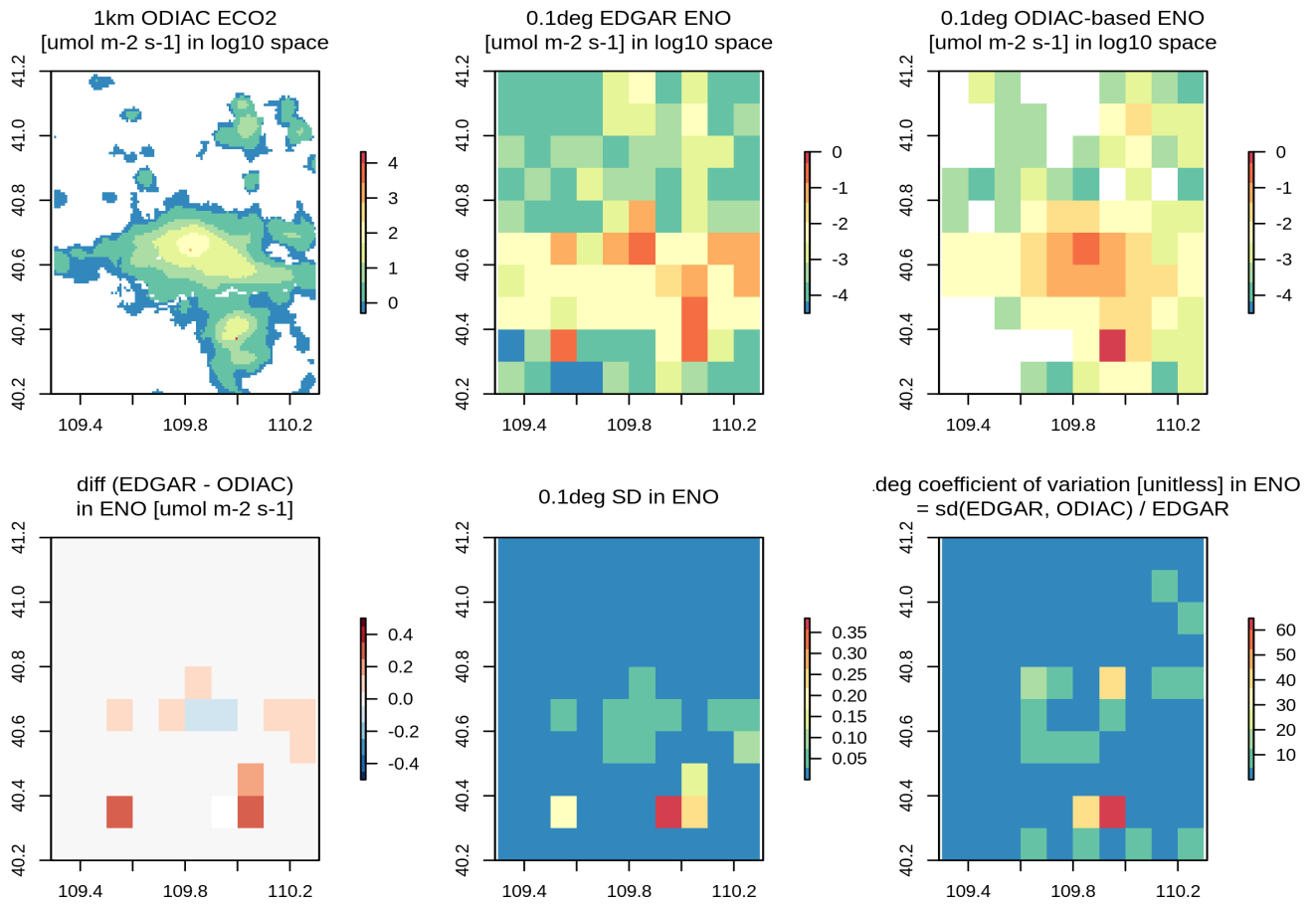


Figure S4. A demonstration of how prior emissions in NO_x can be approximated over Baotou, China. For example, we adopted the CO_2 emissions from ODIAC and the NO -to- CO_2 emission ratios from EDGAR to generate ODIAC-based NO_x emissions. The percent difference between the ODIAC-derived and EDGAR-based NO_x emissions can serve as prior emission uncertainty.

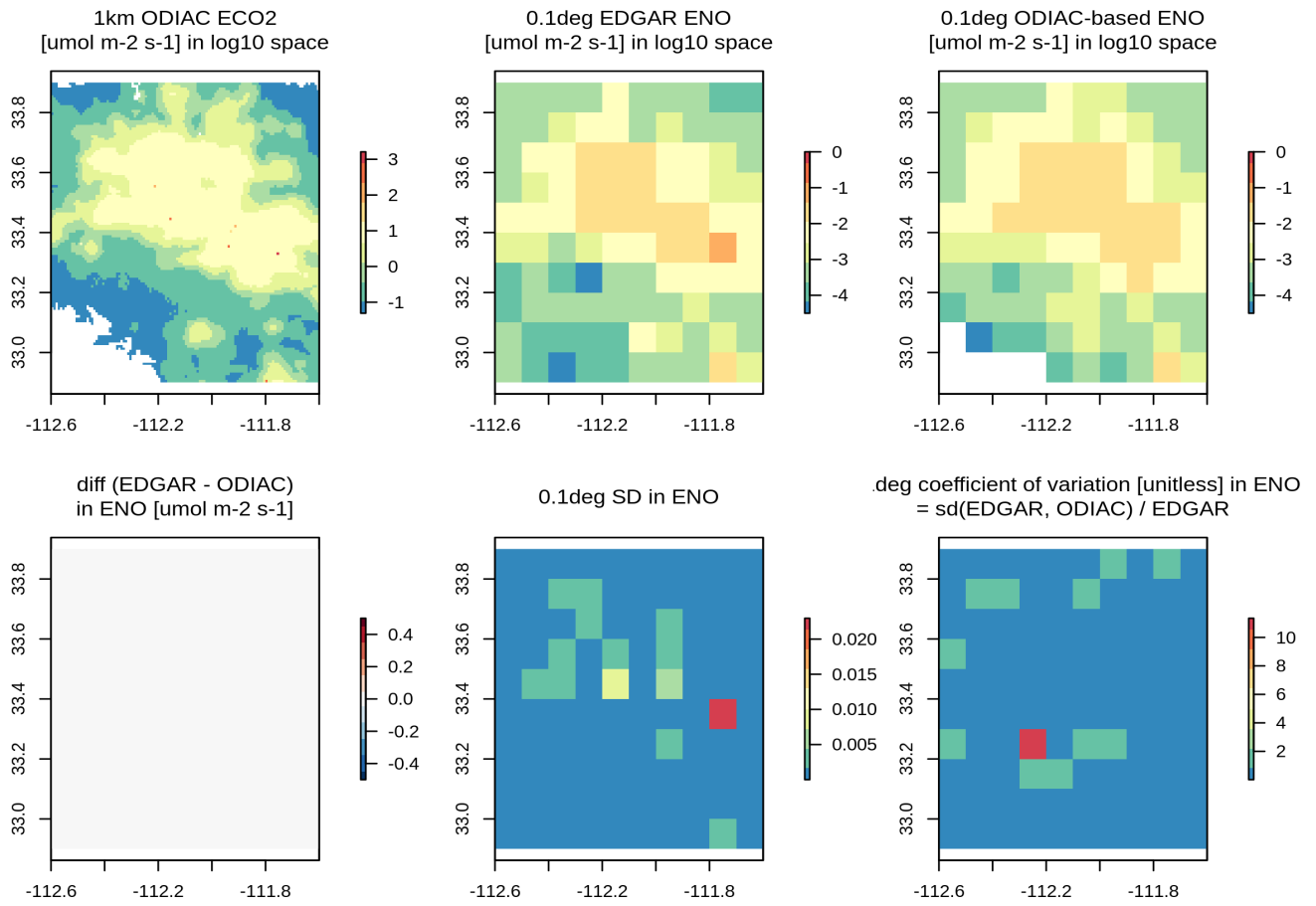


Figure S5. Same as Fig. S4 but over Phoenix, USA. The prior uncertainty over Phoenix is much smaller than that over Baotou (Fig. S4).

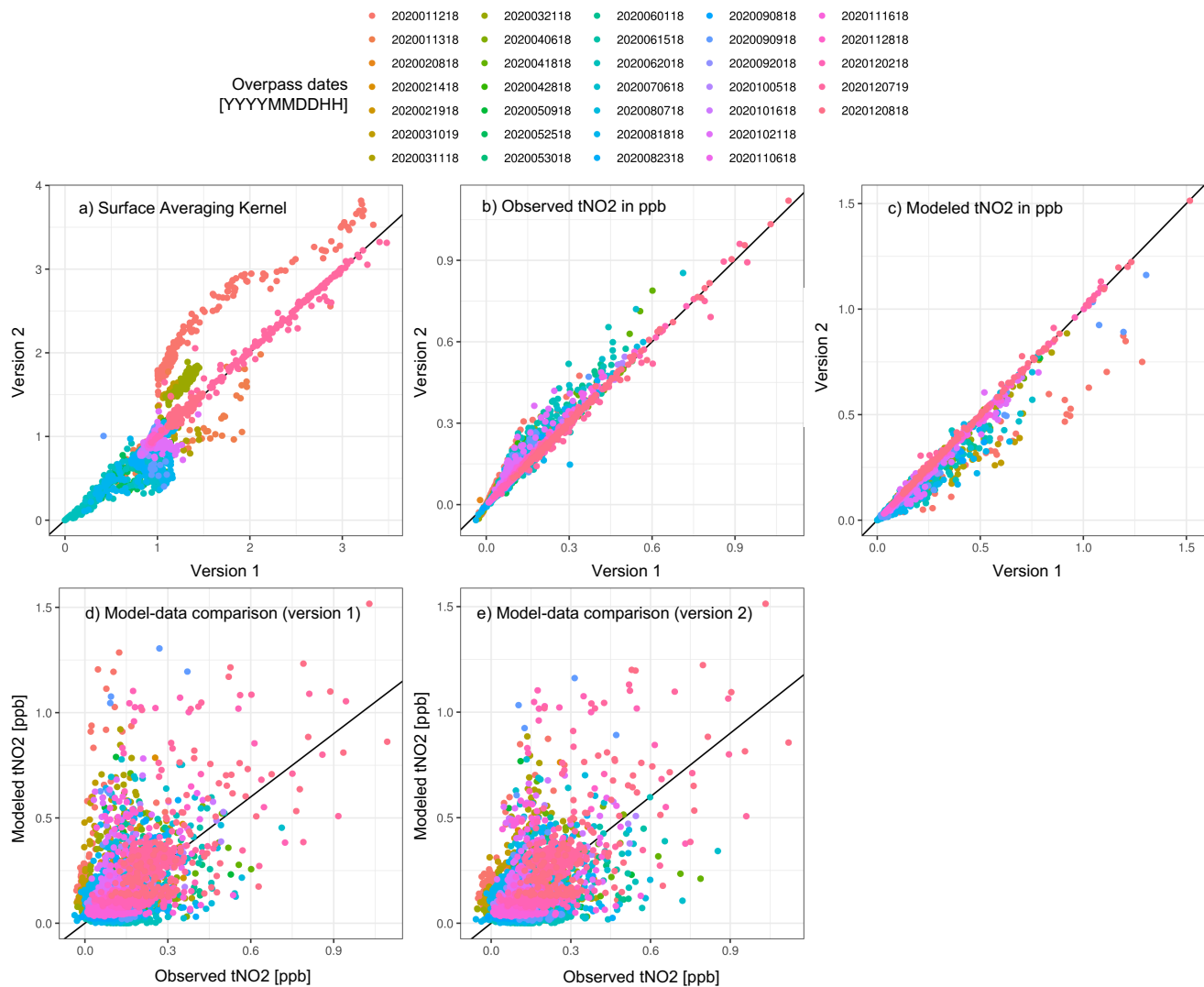


Figure S6. A summary of the differences between TROPOMI v1.3 and v2.3 over soundings around the New Madrid power plant for dozens of overpasses across seasons. Differences in (a) surface-level averaging kernel of tropospheric NO_2 [unitless], (b) observed tNO_2 [ppb], (c) simulated tNO_2 using version-specific AK profiles, and (d,e) model-data comparisons between two versions (v1 vs. v2) are shown, respectively. Color differentiates overpasses and each dot represents one satellite sounding.

Hourly emissions from EPA vs. monthly emissions from EDGARv5 and v6 over US power plants

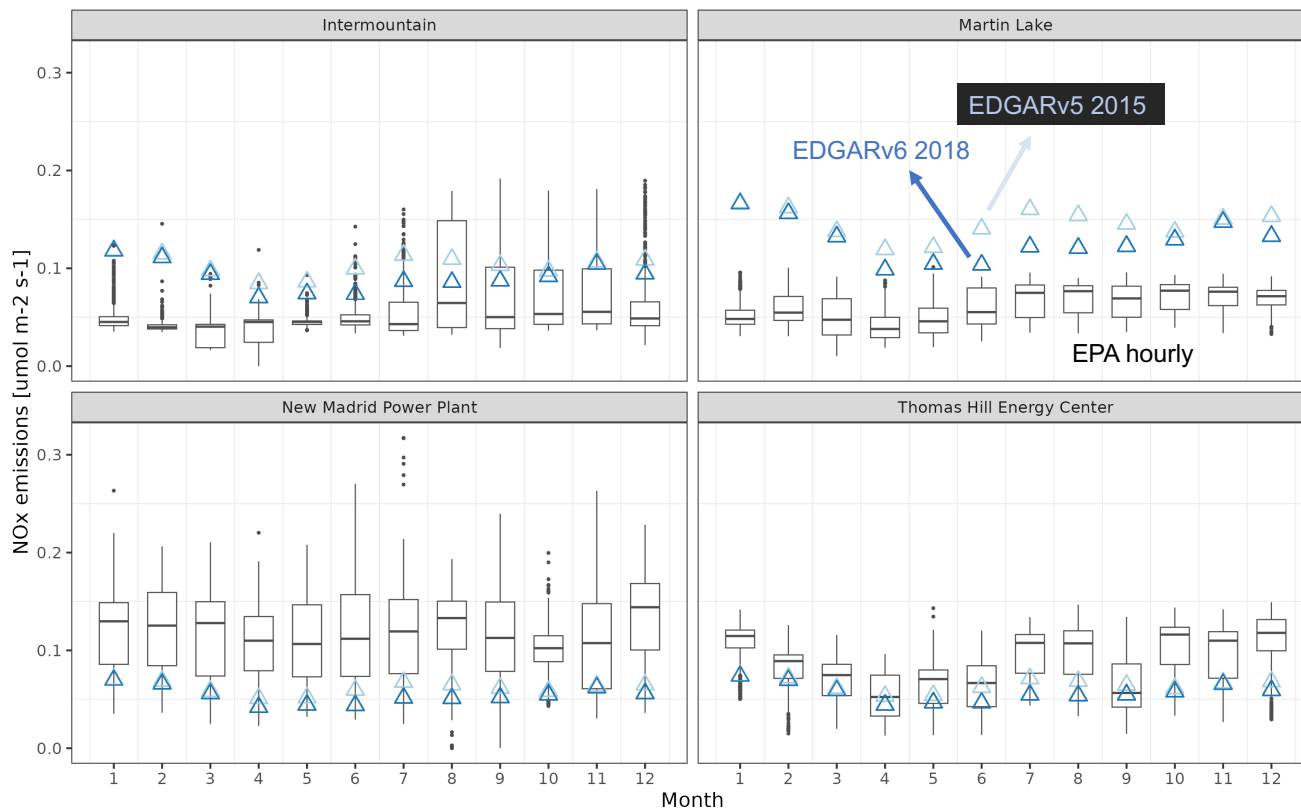


Figure S7. Reported hourly NO_x emissions in 2020 from EPA (black boxplot) [$\mu\text{mol m}^{-2} \text{s}^{-1}$] and monthly mean NO_x emissions from EDGARv5 (with the latest year available of 2015, light blue triangles) and v6 (with the latest year available of 2018, dark blue triangles) for examined power plants.

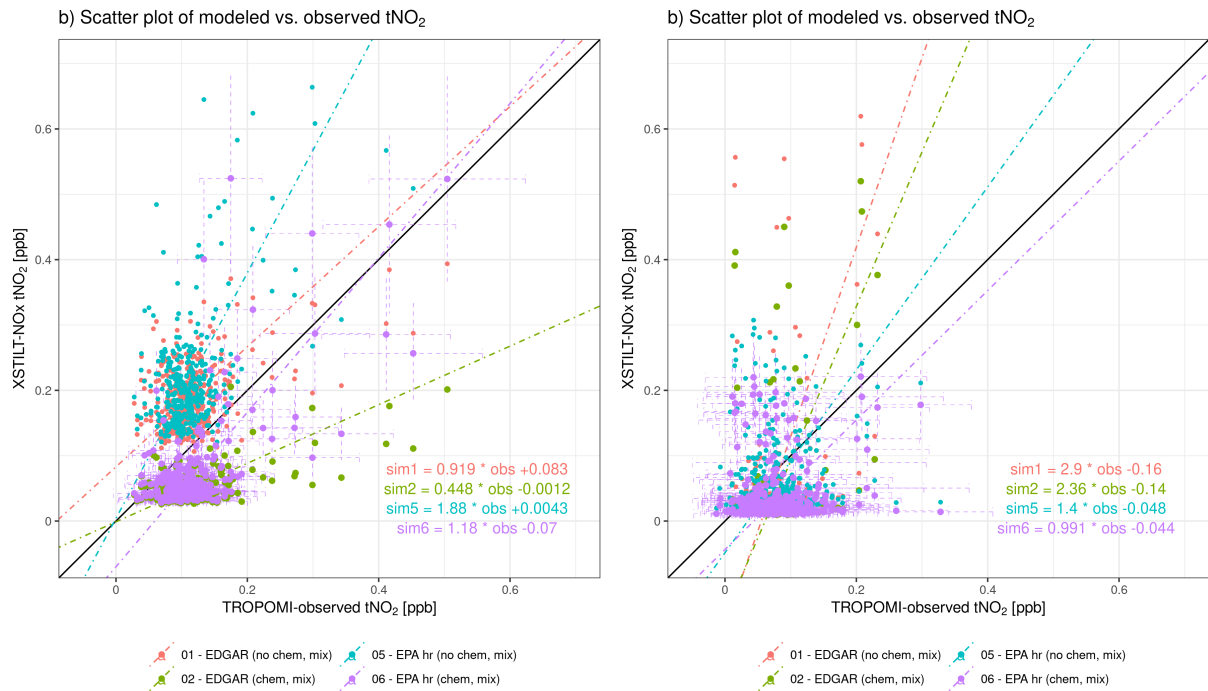


Figure S8. A scatter plot for the model-data comparison over the New Madrid power plant on June 15, 2020, and over the Intermountain power plant on Dec 14, 2020, based on TROPOMI v1.3 data. A similar comparison using TROPOMI v2.3 is presented in Fig. 6. Each dot denotes one satellite sounding. Only four GFS-based simulations using EDGAR without or with lifetime (red/green), and hourly EPA without or with lifetime (blue/purple) are included in the scatter plot. Linear regression fit with the Standardized Major Axis (SMA) solution is performed on the model-data pairs based on four select model configurations (dashed-dotted lines). The 1:1 line is displayed as a solid black line.

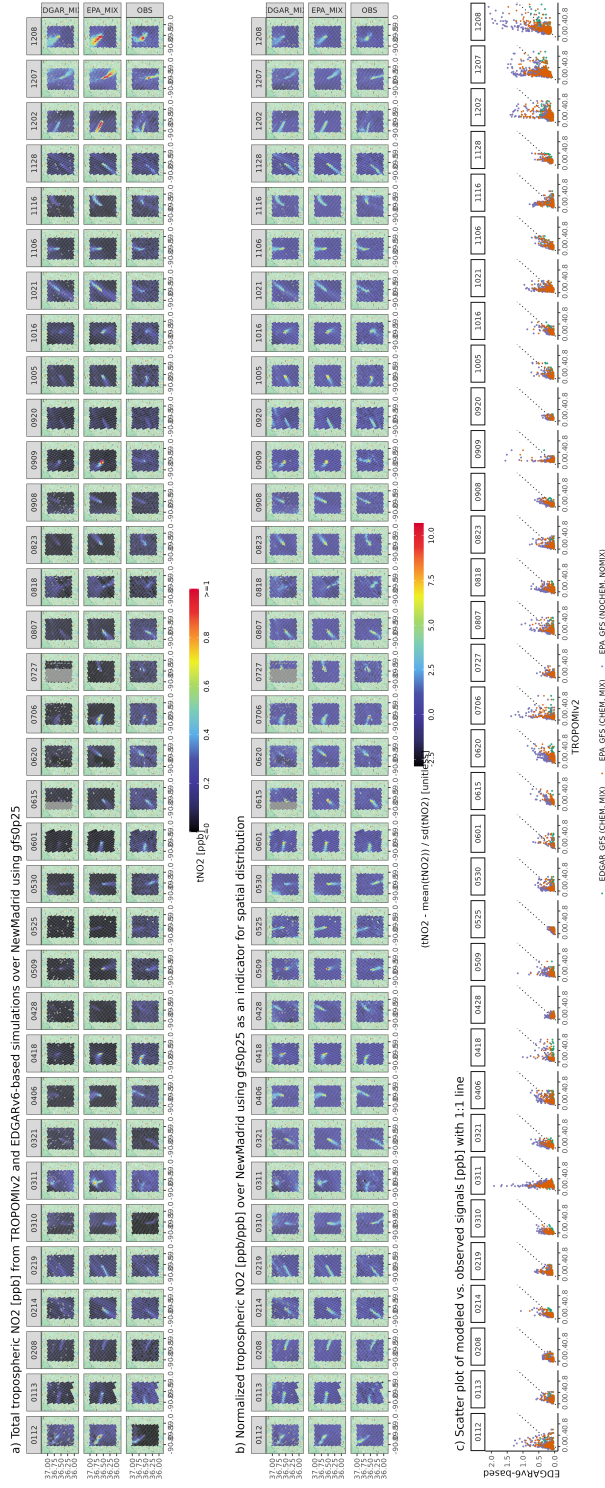


Figure S9. Model-data comparisons for all 34 overpasses around the New Madrid power plant using GFS0p25 as the meteorological field. Top panels: total tropospheric NO₂ from TROPOMIV2 and EDGARv6-based simulations. Middle panels: Standardized signals by first subtracting the spatial average and then normalized by the standard deviations (i.e., z-scores, $[\text{tNO}_2 - \text{mean}(\text{tNO}_2)] / \text{sd}(\text{tNO}_2)$, unitless). Bottom panels: Scatter plot of the model-data comparisons, including EDGARv6-derived simulations with NO_x chemistry (dark green) and EPA-derived simulations with (orange) and without NO_x chemistry (purple).

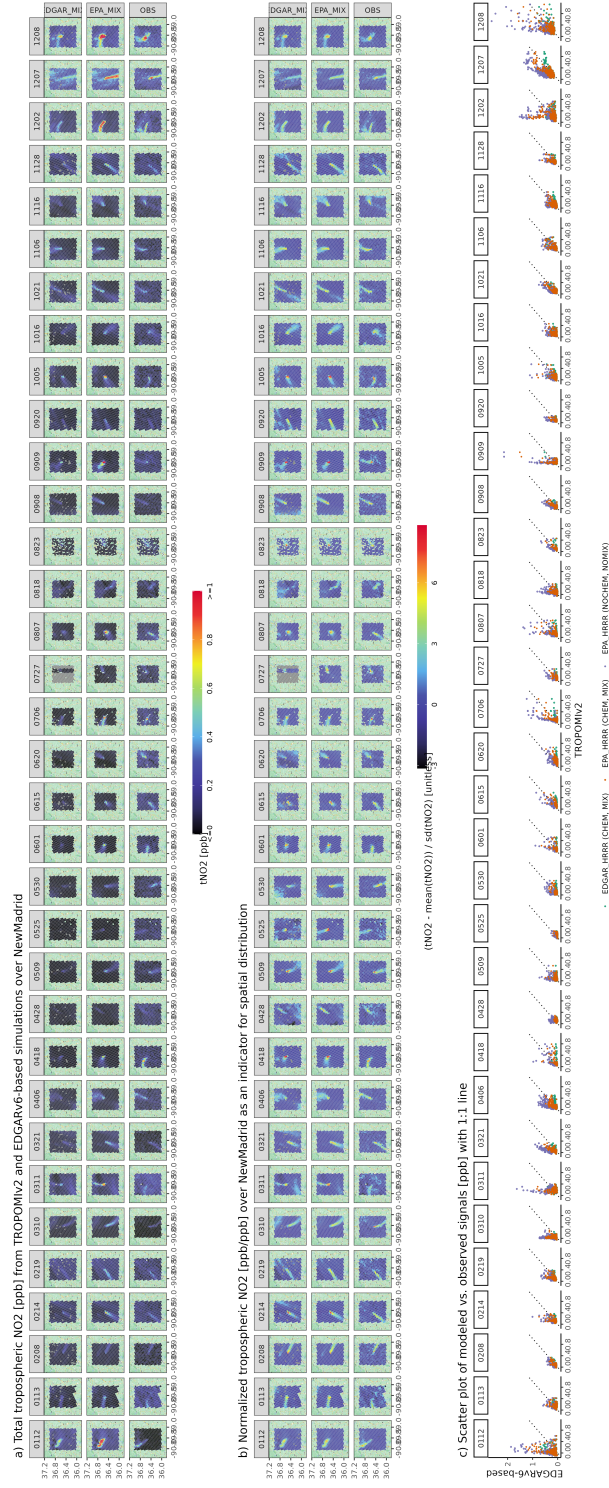
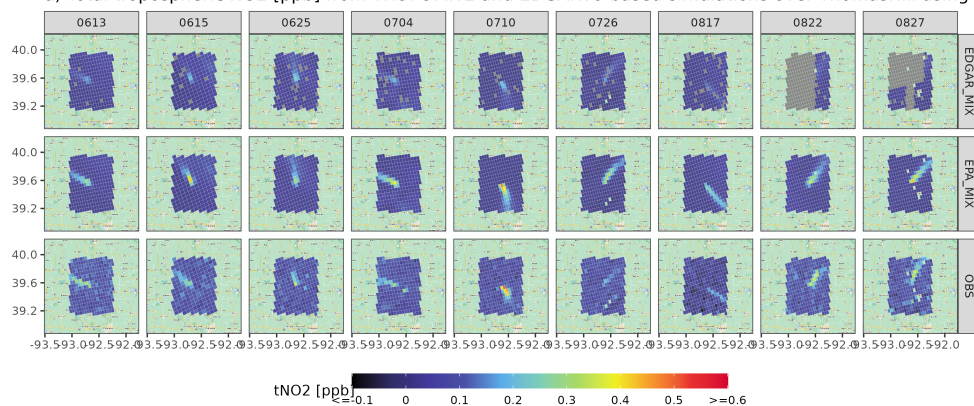
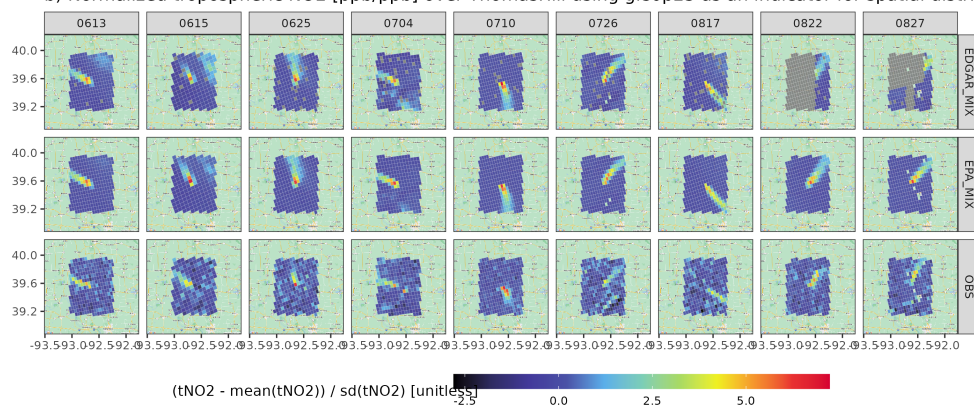


Figure S10. Same model-data comparisons as Fig. S9 around the New Madrid power plant, but for simulations using HRRR as the meteorological field.

a) Total tropospheric NO₂ [ppb] from TROPOMIv2 and EDGARv6-based simulations over ThomasHill using gfs0p25



b) Normalized tropospheric NO₂ [ppb/ppb] over ThomasHill using gfs0p25 as an indicator for spatial distribution



c) Scatter plot of modeled vs. observed signals [ppb] with 1:1 line

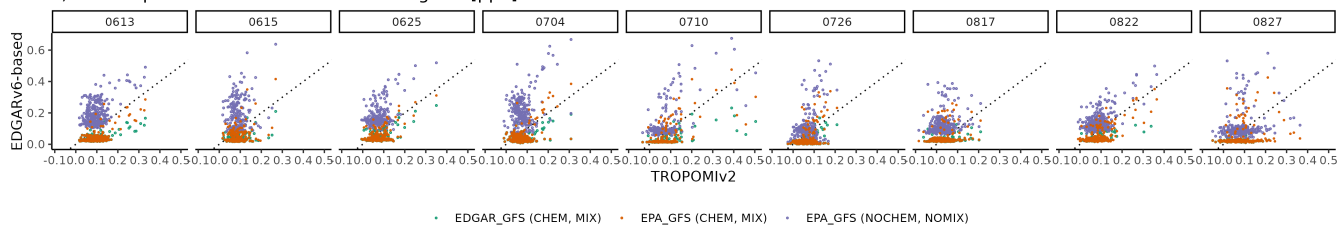
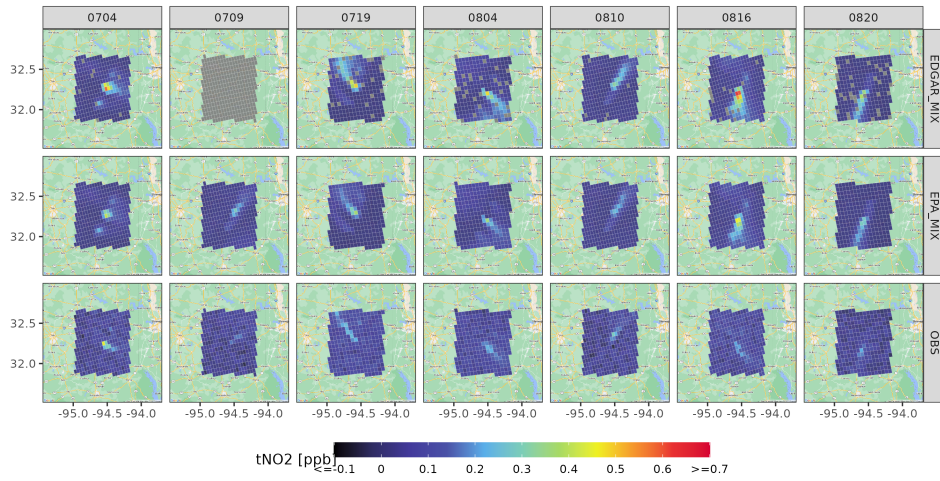
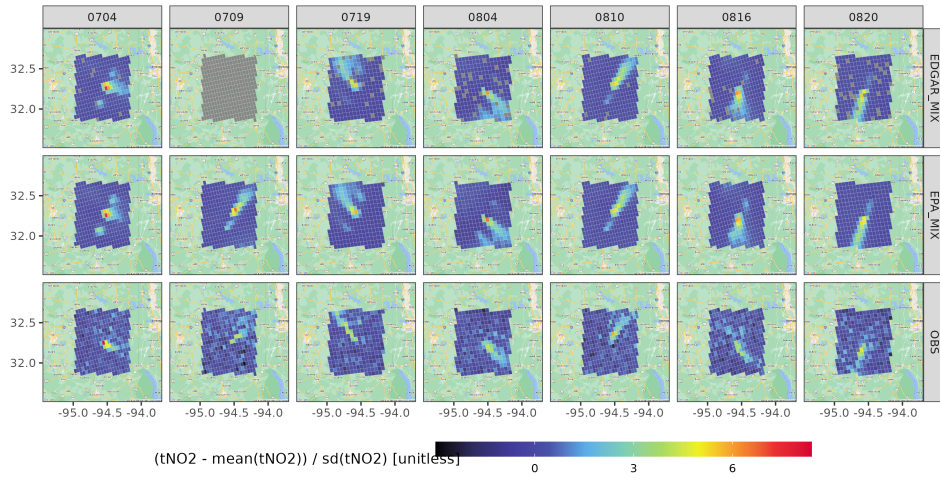


Figure S11. Same model-data comparisons as Fig. S9, but for simulations over the Thomas Hill power plant using GFS as the meteorological field.

a) Total tropospheric NO₂ [ppb] from TROPOMIv2 and EDGARv6-based simulations over MartinLake using gfs0p25



b) Normalized tropospheric NO₂ [ppb/ppb] over MartinLake using gfs0p25 as an indicator for spatial distribution



c) Scatter plot of modeled vs. observed signals [ppb] with 1:1 line

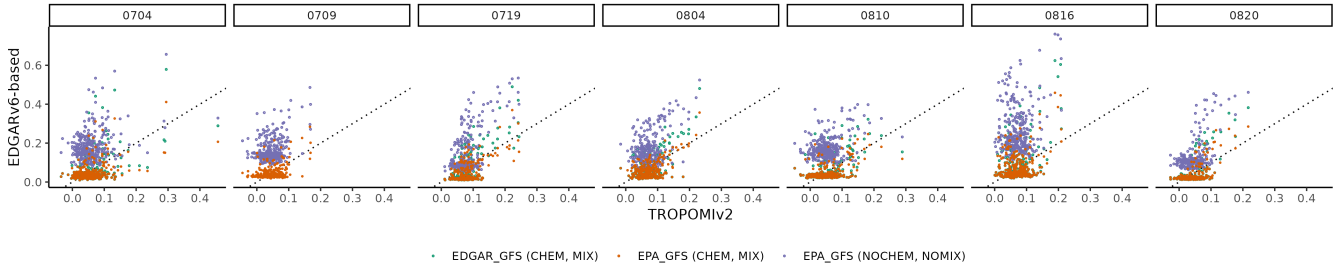


Figure S12. Same model-data comparisons as Fig. S9, but for simulations over the Martin Lake power plant using GFS as the meteorological field.

Model-data slope using both v1.3 and v2.3 of TROPOMI data over all power plants per TROPOMI overpass

Config: NOCHEM vs. CHEM; EDGAR vs. EPA; GFS vs. HRRR

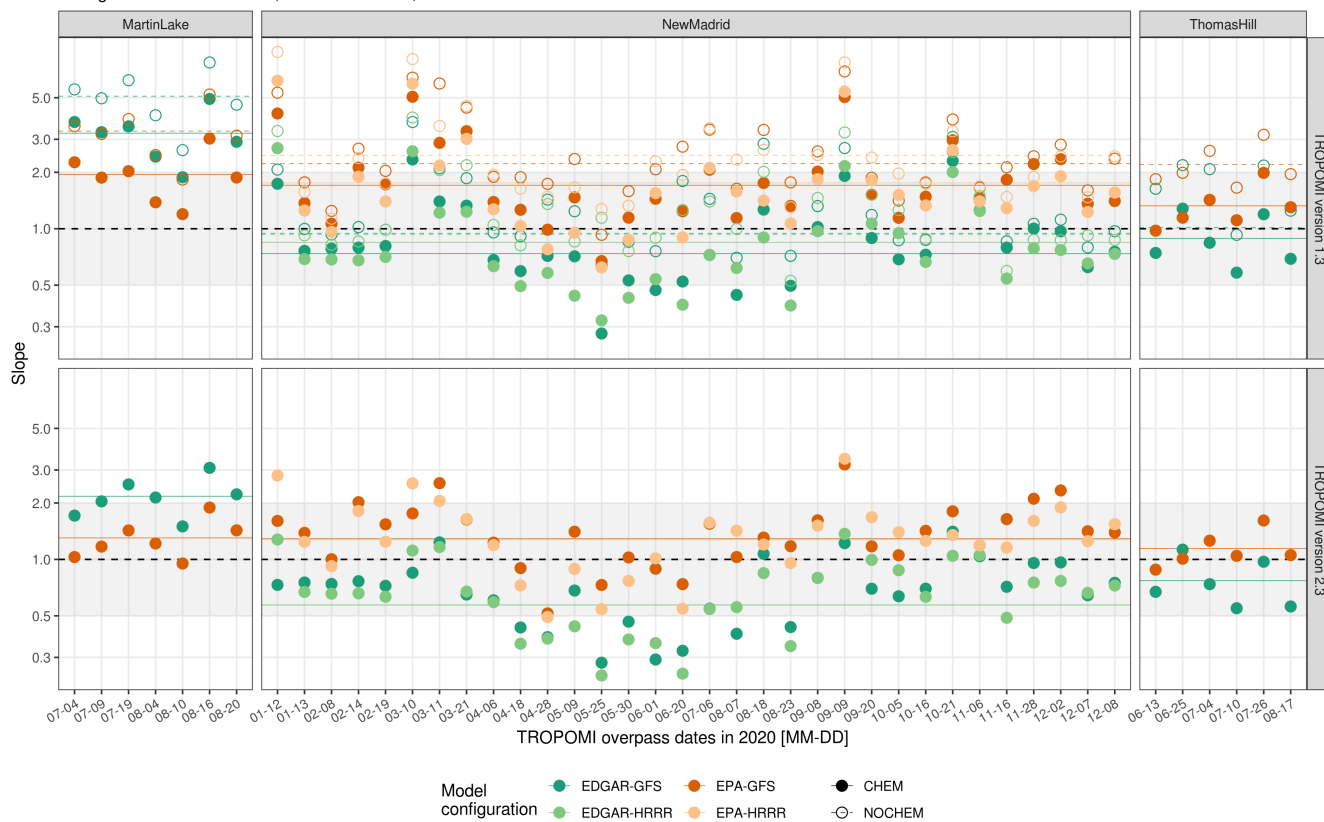


Figure S13. Same as Fig. 6, but the observations are obtained from both TROPOMI v1.3 and v2.3, while the simulations are carried out using annual mean EDGARv5.0 with the latest year available of 2015.

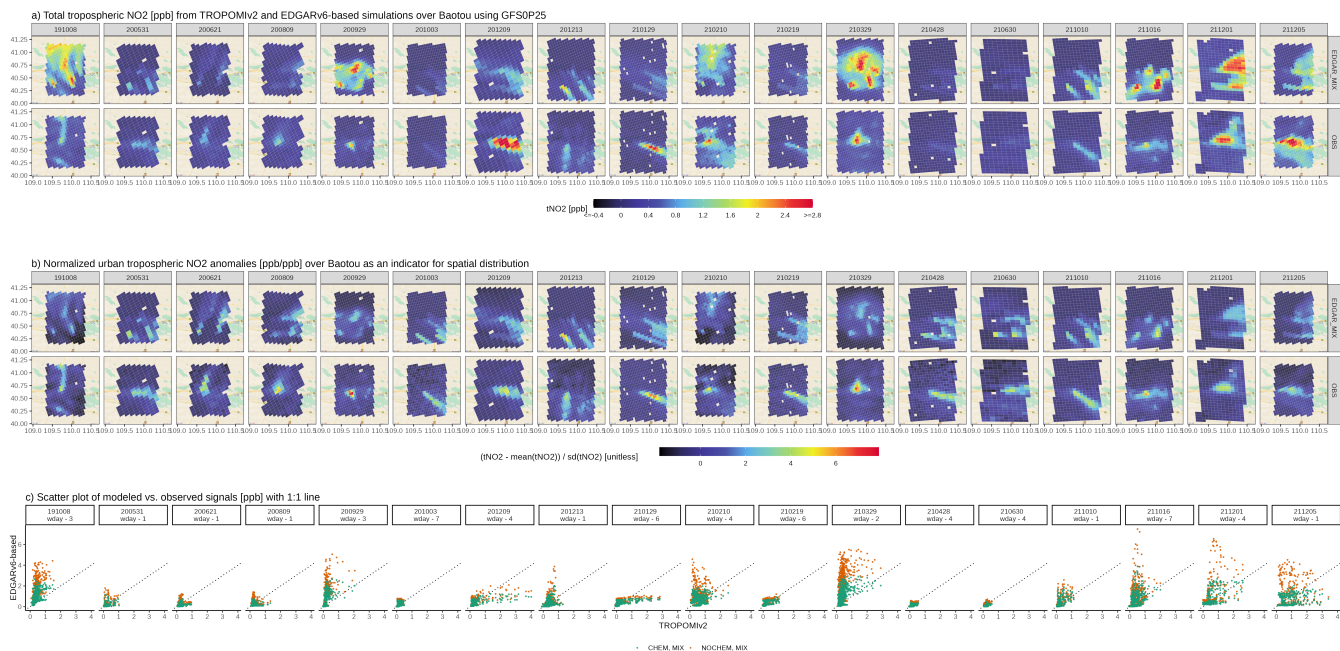


Figure S14. Examples of GFS/EDGARv6-derived and TROPOMIv2-based tNO₂ plumes over Baotou. Modeled plumes are generated using annual mean ENO_x from EDGAR with top emitters highlighted in light-grey circles. XCO₂ enhancements calculated from a local background have been averaged based on the TROPOMI sounding size. Only 18 TROPOMI overpasses that coincide with OCO-3 overpasses with time differences of < 1 hour are shown here.

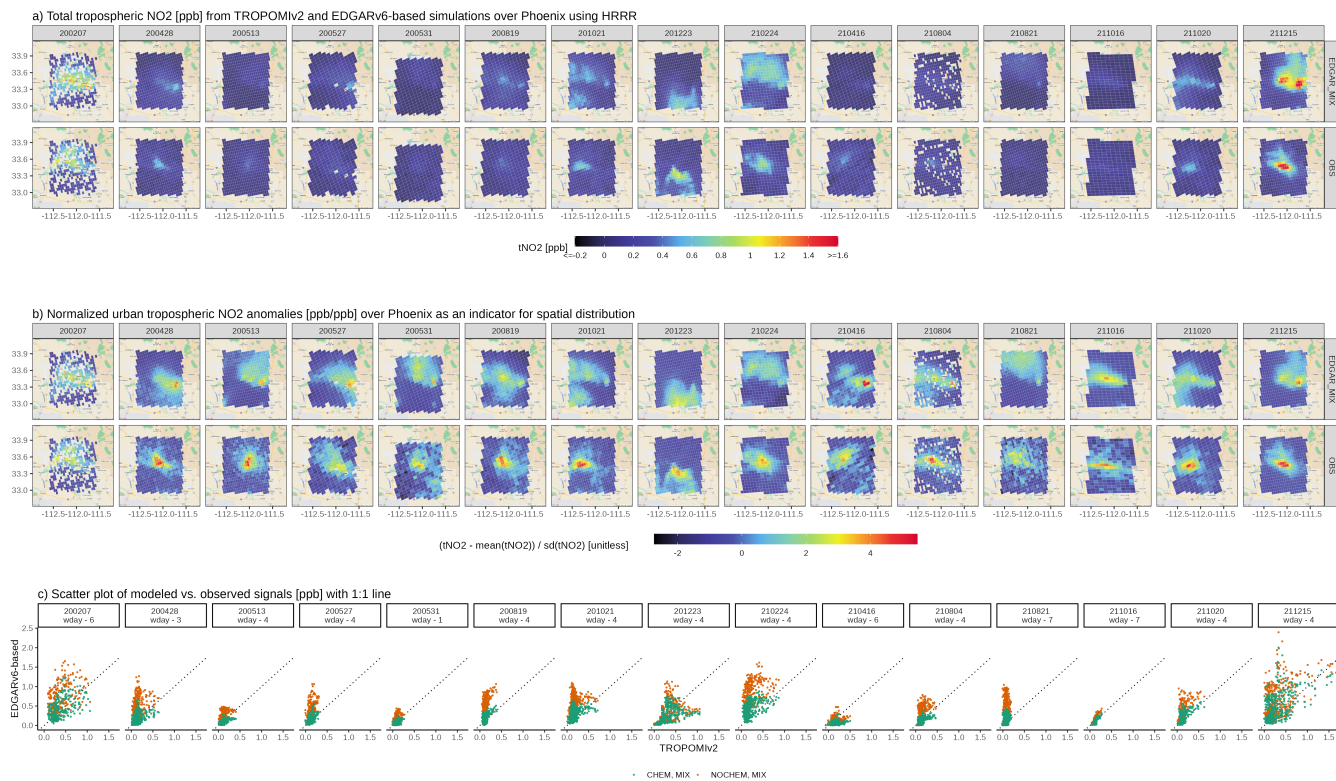


Figure S15. Same as **Fig. S14**, but over Phoenix. Only 15 TROPOMI overpasses that coincide with OCO-2 and OCO-3 overpasses with time differences of < 1 hour are shown here.

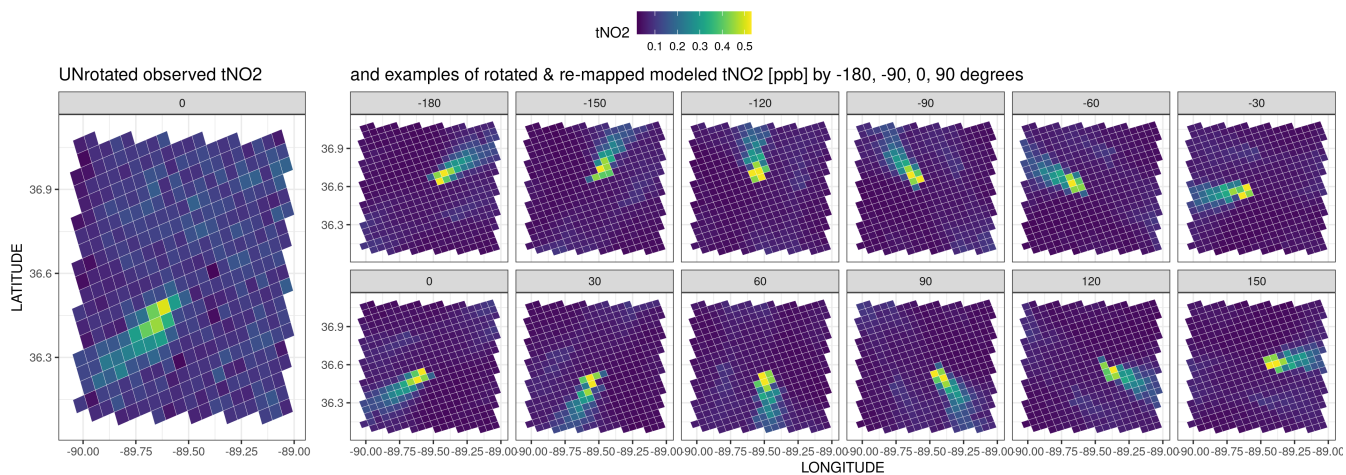


Figure S16. A demonstration of how modeled plume is rotated and re-mapped to the original TROPOMI pixels using $t\text{NO}_2$ simulations on June 15, 2020, over the New Madrid power plant. Observed $t\text{NO}_2$ on TROPOMI grids (upper left) and modeled $t\text{NO}_2$ plumes with multiple rotation angles are plotted.

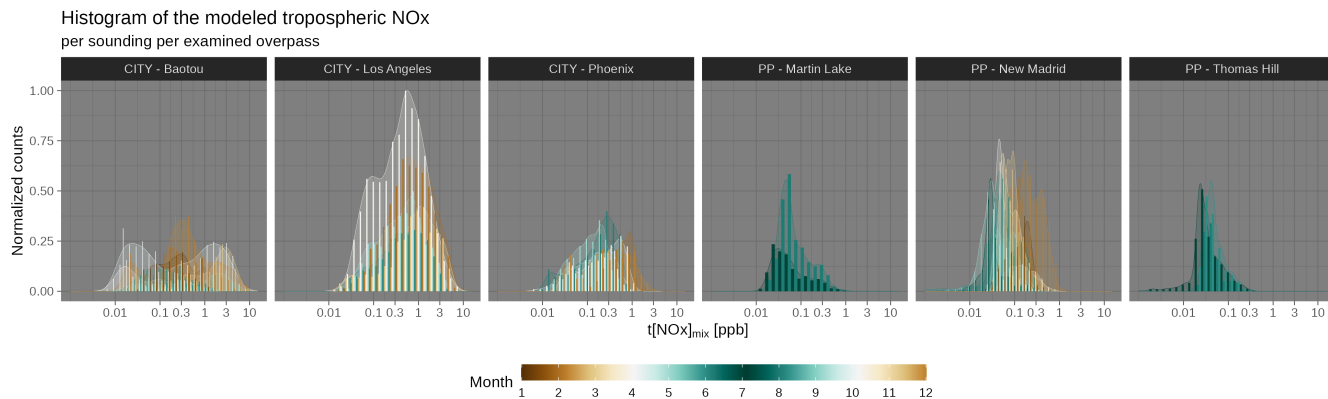


Figure S17. A histogram of the modeled tropospheric NO_x [ppb] for every TROPOMI sounding from all overpasses and all sites.

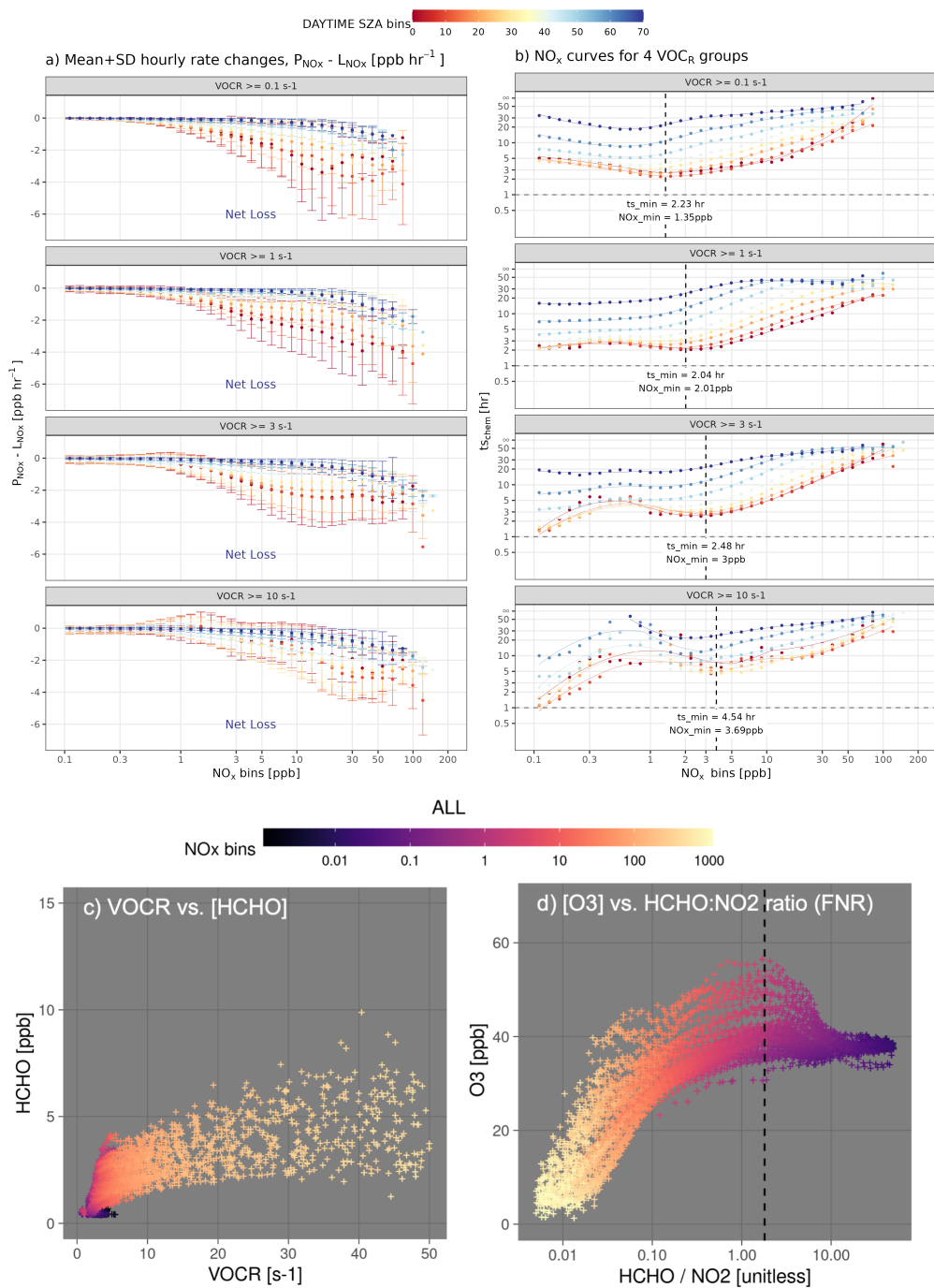


Figure S18. (ab) Similar to Fig. 3ab, but differentiated by three intervals of VOCR_R and for selected SZAs intervals with a spacing of 10 degrees. All panels utilized model results from the same WRF-Chem simulations described in Appendix A. (cd) Relations of HCHO concentration [ppb] with VOCR_R [s⁻¹] and O₃ concentration [ppb] with HCHO:NO₂ ratio (FNR) with color gradient denoting modeled NO_x concentrations. All panels utilized model results from the same WRF-Chem simulations described in Sect. 2 and Appendix A.

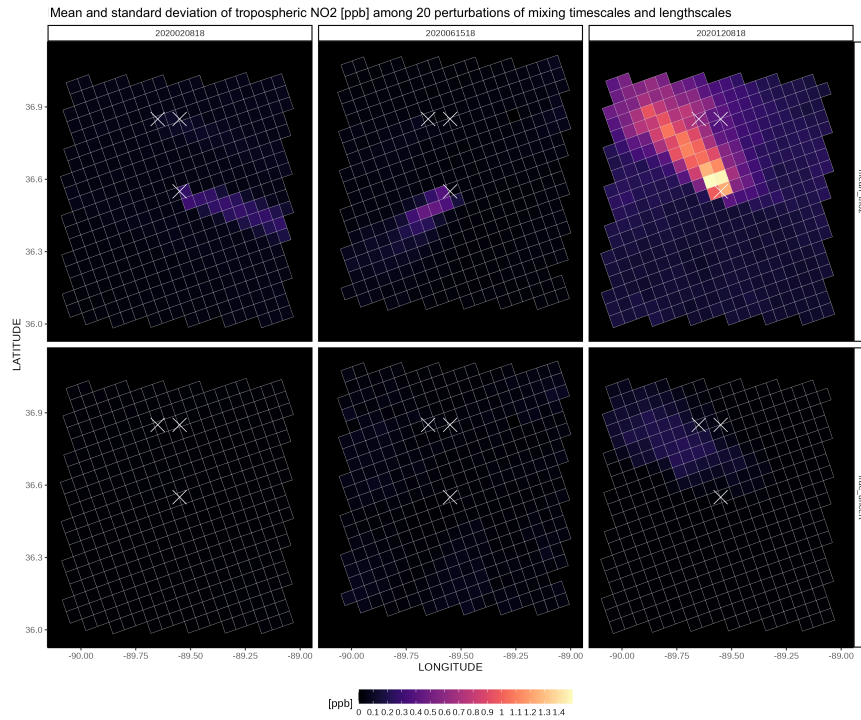


Figure S19. Mean and standard deviation of modeled tNO₂ for three TROPOMI overpasses (Feb 8, June 15, and Dec 8, 2020) over the New Madrid power plant using various horizontal mixing length scales (i.e., 0.5, 1, 3, 6, 12 km) and timescales (i.e., 0.5, 1, 6, 12 hours).

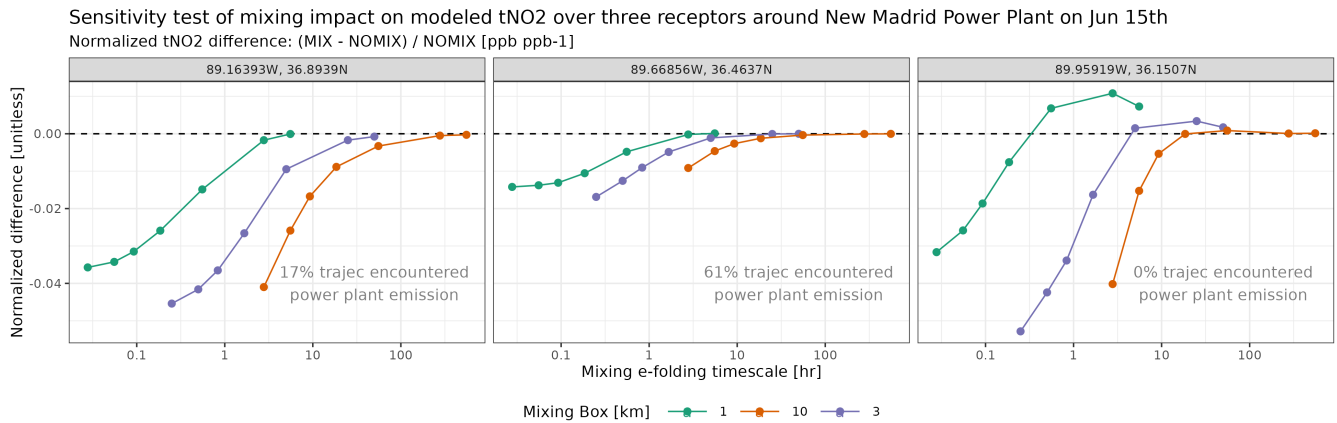


Figure S20. Normalized difference in modeled tropospheric NO₂ between the mixing and non-mixing runs as a function of the horizontal mixing timescale [hr, x-axis] and mixing length scale [km, in colors]. The normalized difference is calculated as $(tNO_{2,MIX} - tNO_{2,NOMIX}) / tNO_{2,NOMIX}$. Three examples for three receptors/soundings on June 15th for the New Madrid case are shown here and they differ by the fraction of model trajectories that “hit” the power plant emission. For receptors where some trajectories encountered the emissions, a faster mixing reducing the spatial gradient in NO_x leads to a reduced final tNO₂ at the receptor (left two panels).